

INFORMATION ON THE NUCLEAR PERIPHERY
FROM ANTIPROTONIC ATOMS*

A. TRZCIŃSKA, J. JASTRZĘBSKI, P. LUBIŃSKI

Heavy Ion Laboratory, Warsaw University
Pasteura 5A, 02-093 Warsaw, Poland

F.J. HARTMANN, R. SCHMIDT, T. VON EGIDY

Physik-Department, Technische Universität München
85747 Garching, Germany

AND B. KŁOS

Institute of Physics, University of Silesia
40-007 Katowice, Poland*(Received November 21, 2000)*

In the PS209 experiments at CERN two kinds of measurements were performed: the in-beam measurement of X-rays from antiprotonic atoms and the radiochemical, off-line determination of the yield of annihilation products with mass number $A_t - 1$ (less by 1 than the target mass). Both methods give observables which allows to study the peripheral matter density composition and distribution. A comparisons of the PS209 results with the theoretical and semiempirical predictions for neutron and proton densities and with the differences Δr_{np} of the rms radii of neutrons and protons obtained in other experiments are also presented.

PACS numbers: 36.10.-k, 21.10.Gv, 13.75.Cs

Antiprotons are a convenient tool for the investigation of the nuclear surface. The \bar{p} -nucleus interaction has peripheral character and even a small overlap between antiprotonic and nuclear wave functions is sufficient to reveal the influence of the strong interaction. The strong interaction reduces the lifetime of the lowest levels in the antiprotonic atom reached during

* Presented at the XXXV Zakopane School of Physics "Trends in Nuclear Physics", Zakopane, Poland, September 5-13, 2000.

the cascade (the levels become wider) and shifts them from purely electromagnetic energy. To first approximation the strong interaction potential is proportional to the nuclear matter density [1]. Therefore the widths and shifts of last levels, which depend on this potential, can give information on the density at the nuclear periphery where the annihilation takes place, or — more precisely — at a distance about $R_{1/2} + 1.5$ fm (where $R_{1/2}$ is the half-density charge radius), as calculations indicate [2].

The PS209 experiment, performed at LEAR (CERN), aimed at the determination of level widths and shifts caused by the strong interaction through the measurements of the X-rays from antiprotonic atoms. These observables were measured for 55 isotopes. At present 44 level shifts, 29 “lower” level widths and 33 “upper” level widths are determined [3] (comp. figure 1).

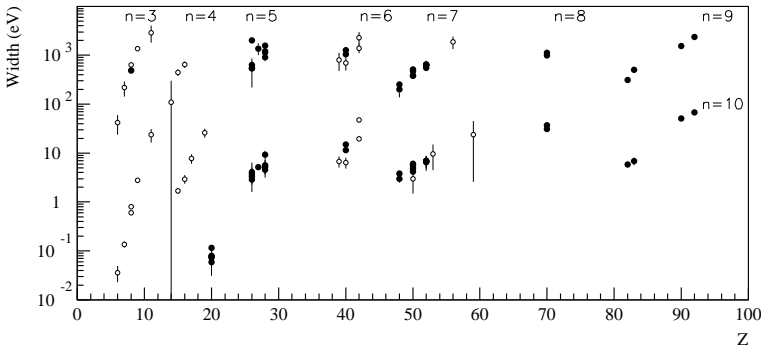


Fig. 1. Antiprotonic strong interaction level widths as a function of atomic number Z . Full circles — values determined in PS209 experiment; open circles — earlier data [4].

Studying the products of the annihilation process gives us an information on the density distribution about 1 fm further than the antiprotonic X-rays method do. Part of the beam time of the PS209 experiment was used for the continuation of the radiochemical measurements [5, 6] consisting in the determination of the annihilation residues with mass number one unit smaller than the target mass A_t . When the products with neutron number $N_t - 1$ and products with proton number $Z_t - 1$ are radioactive it is easy to determine their relative yields with standard nuclear-spectroscopy methods. These yields are directly related to the proton and neutron densities at the annihilation site. The yields were transformed to the halo factor f_{halo} defined by

$$f_{\text{halo}} = \frac{N(\bar{p}n)}{N(\bar{p}p)} \frac{Z \operatorname{Im}(a_p)}{N \operatorname{Im}(a_n)}, \quad (1)$$

where the first term is the yield ratio of the products $A_t - 1$, the second term is the normalization factor and the third term — the ratio of the imaginary

parts of the antiproton–nucleon scattering amplitudes — expresses the ratio of annihilation probability on a proton to that on a neutron. The halo factor defined above is proportional to the neutron to proton density ratio ρ_n/ρ_p at the annihilation site. For a quantitative comparison of ρ_n/ρ_p with the values derived from f_{halo} one should take into account that the probability for annihilation leading to $A_i - 1$ (the so called “cold” annihilations) is non-zero in an extended region (with FWHM of about 2-3 fm) [2]. Within this publication f_{halo} is assumed to represent ρ_n/ρ_p at the most probable site of “cold” annihilations — at a distance $R_{1/2} + 2.5 \pm 0.5$ fm. It was proven for several cases that such a simplified presentation does not introduce errors larger than 10%–15%.

The results obtained with the radiochemical method were already published [7, 8]. A strong negative correlation between the halo factor and neutron separation energy B_n was observed. The halo factor is larger than one for nuclei with $B_n \lesssim 9$ MeV: for these isotopes the nuclear periphery is rich in neutrons.

It is interesting to compare the results of our radiochemical measurements with data from other experiments investigating differences between neutron and proton distributions. Figure 2 compares values of halo factor and ρ_n/ρ_p deduced from Δr_{np} — neutron and proton differences of rms (root mean squared) radii. In order to “translate” Δr_{np} into density ratios a two parameter Fermi (2pF) distribution was assumed for the proton as well as for the neutron density. The charge distribution parameters determined from muonic atoms experiments or from electron scattering were taken from tables [14, 15]. These parameters were converted to proton distribution parameters (c_p, a_p) according to a prescription given by Oset [16]. Having $\Delta r_{np} = r_n(c_n, a_n) - r_p(c_p, a_p)$ one may consider two extreme cases: (a) $a_n = a_p$; $c_n \neq c_p$ — a “neutron skin” model or (b) $a_n \neq a_p$; $c_n = c_p$ — a “neutron halo” model. It is seen from Fig. 2 that the f_{halo} data clearly favour the “neutron halo” model. (It is worth to note that assuming cases with $a_n \neq a_p$ and $c_n \neq c_p$ leads to values between the full and dashed lines in Fig. 2.)

The results of the radiochemical method were also compared with prediction of the Hartree–Fock–Bogoliubov (HFB) [17] calculations and with the semiempirical formulae for $\rho_p(r)$ and $\rho_n(r)$ proposed by Gambhir and Patil [18]. Figure 3 shows examples. Values for $Z/N \rho_p(r)/\rho_n(r)$ derived from our f_{halo} measurements are compared with those deduced from these two theories. Good agreement was obtained for 15 isotopes (of 19 measured f_{halo} cases). For ^{96}Ru , ^{106}Cd , ^{112}Sn and ^{144}Sm the experimental values are significantly smaller than the theoretical ones. An explanation was proposed recently [19].

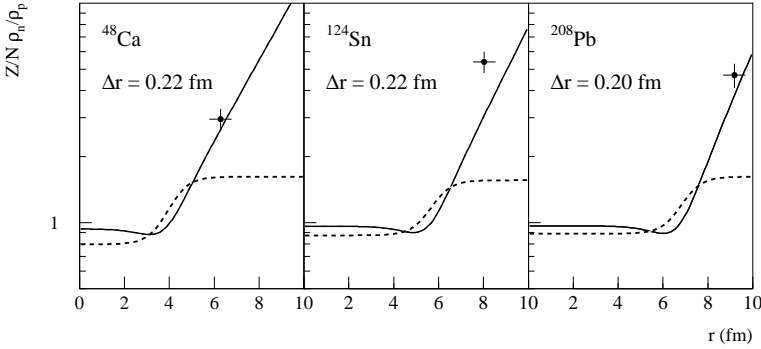


Fig. 2. Comparison of the normalized neutron to proton density ratio deduced from Δr_{np} data for ^{48}Ca [4], ^{124}Sn [4, 9, 10] and ^{208}Pb [9, 11] with f_{halo} — marked with crosses at the most probable annihilation site ($\frac{\int_0^{f_{\text{halo}}} a(\bar{p}n)}{\int_0^{f_{\text{halo}}} a(\bar{p}p)}$) taken to be equal 0.63 [12, 13]). Solid line: neutron to proton density ratio deduced from Δr_{np} under the assumption of $c_n = c_p$ (“neutron halo” model), dashed line $a_n = a_p$ assumed (“neutron skin” model).

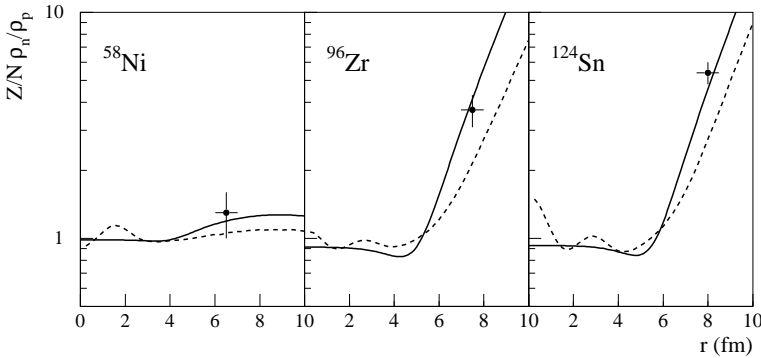


Fig. 3. Examples of normalized neutron to proton density ratio calculated with the HFB method — dashed lines — and the semiempirical formula of Gambhir and Patil — solid lines. Crosses indicate the measured f_{halo} .

As it was mentioned already earlier, the information on neutron density distribution may also be deduced from the X-rays measurements. If one assumes that the proton density distribution is well determined (from experiments using electromagnetically interacting probes) and the strong interaction potential is known, neutron density parameters are the only “free” variables in the fit of the matter distribution to the observed levels widths and shifts in antiprotonic atoms. 2pF distributions and modified Batty optical potential [1] were considered in analysis (for details see [20]) and $c_n = c_p$ was assumed — justified by the better agreement of the f_{halo} and Δr_{np} data

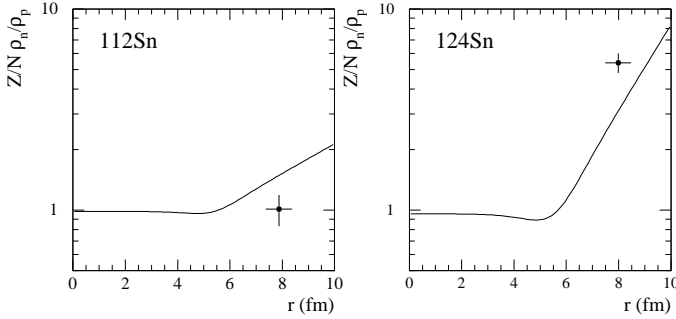


Fig. 4. Comparison of f_{halo} (crosses) and neutron to proton density ratio deduced from X-rays measurement (modified Batty potential [1] with $\frac{\text{Im } \alpha(\bar{p}n)}{\text{Im } \alpha(\bar{p}p)} = 0.63$ was used). The halo factor is marked at radial distance $R_{1/2} + 2.5$ fm.

(see above). Figure 4 presents the comparison of $Z/N \rho_n/\rho_p$ determined from the strong interaction widths and shifts with f_{halo} for Sn isotopes. Although a qualitative agreement between the two methods is evident, quantitative agreement is not reached. Similar problems were encountered in other nuclei, $^{128,130}\text{Te}$ [21] and ^{176}Yb [22]. Possible explanations are that the 2pF distribution does not describe properly the outermost nuclear periphery or that the adopted \bar{p} -nucleus potential [1] is not valid for heavy elements. On the other hand the parameters of the nuclear matter distribution obtained from X-ray data give neutron and proton rms radius differences which are in very good agreement with the Δr_{np} obtained in other experiments — see Fig. 5.

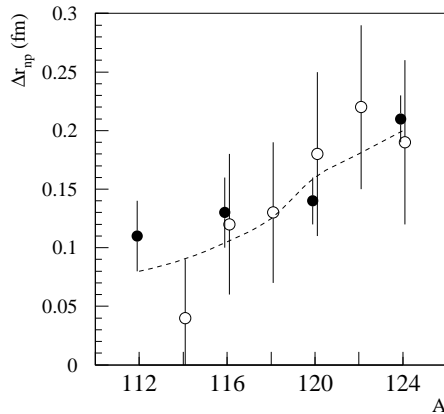


Fig. 5. Comparison of Δr_{np} values for Sn isotopes calculated with parameters of nuclear matter distribution obtained from X-rays data (full circles) and Δr_{np} measurements [10] (open circles). Theoretical prediction of HFB calculations [23] is also drawn (dashed line).

In conclusion, based on a few examples from much more abundant antiprotonic atom and radiochemical data we have shown that:

- the radiochemical results clearly favour the peripheral neutron distribution in the form of a “neutron halo” rather than of a “neutron skin” type;
- the in-beam antiprotonic X-ray measurement combined with the proton distributions gathered from electron scattering or muonic atom experiments give a new way for the determination of the peripheral neutron distribution in nuclei;
- the differences between the neutron and proton rms radii obtained from antiprotonic X-rays and from other published results are in fair agreement between themselves;
- assuming 2pF density distributions, the peripheral neutron density determined by the radiochemical method is larger than that determined from antiprotonic X-rays data. The different radial distances at which both methods probe the nuclear periphery may be the reason of this discrepancy.

Our thanks are due to Sławomir Wycech for discussions. This work was supported by the Polish State Committee for Scientific Research (KBN) grants 2 P03B 048 15 and 2 P03B 119 16 and by the Deutsche Forschungsgemeinschaft, Bonn.

REFERENCES

- [1] C.J. Batty, E. Friedman, A. Gal, *Phys. Rep.* **287**, 386 (1997).
- [2] S. Wycech, J. Skalski, R. Smolańczuk, J. Dobaczewski, J.R. Rook, *Phys. Rev.* **C54**, 1832 (1996); S. Wycech private communication.
- [3] A. Trzcińska, J. Jastrzębski, T. Czosnyka, T. von Egidy, K. Gulda, F.J. Hartmann, J. Iwanicki, B. Ketzer, M. Kisieliński, B. Kłos, W. Kurcewicz, P. Lubiński, P. Napiorkowski, L. Pieńkowski, R. Schmidt, E. Widmann, *Nucl. Phys. B, Proceedings of the Sixth Biennial Conference on Low-Energy Antiproton Physics, Venice 2000*, to be published.
- [4] C.J. Batty, E. Friedman, H.J. Gils, H. Rebel, in *Advances in Nuclear Physics*, edited by J.W. Negele and E. Vogt, Plenum Press, New York, 1989, Vol.19.
- [5] J. Jastrzębski, H. Daniel, T. von Egidy, A. Grabowska, Y.S. Kim, W. Kurcewicz, P. Lubiński, G. Riepe, W. Schmid, A. Stolarz, S. Wycech, *Nucl. Phys.* **A558**, 405c (1993).

- [6] P. Lubiński, J. Jastrzębski, A. Grochulska, A. Stolarz, A. Trzcińska, W. Kurcewicz, F.J. Hartmann, W. Schmid, T. von Egidy, J. Skalski, R. Smolańczuk, S. Wycech, D. Hilscher, D. Polster, H. Rossner, *Phys. Rev. Lett.* **73**, 3199 (1994).
- [7] P. Lubiński, J. Jastrzębski, A. Trzcińska, W. Kurcewicz, F.J. Hartmann, W. Schmid, T. von Egidy, R. Smolańczuk, S. Wycech, *Phys. Rev.* **C57**, 2962 (1998).
- [8] R. Schmidt, F.J. Hartmann, B. Ketzer, T. von Egidy, T. Czosnyka, J. Jastrzębski, M. Kisieliński, P. Lubiński, P. Napiorkowski, L. Pieńkowski, A. Trzcińska, B. Kłos, R. Smolańczuk, S. Wycech, W. Poschl, K. Gulda, W. Kurcewicz, E. Widmann, *Phys. Rev.* **C60**, 054309 (1999).
- [9] A. Krasznahorkay, A. Balanda, J.A. Bordewijk, S. Brandenburg, M.N. Harakeh, N. Kalantar-Nayestanaki, B.M. Nyako, J. Timar, A. Van der Woude, *Nucl. Phys.* **A567**, 521 (1994).
- [10] A. Krasznahorkay, M. Fujiwara, P. van Aarle, H. Akimune, I. Daito, H. Fujimura, Y. Fujita, M.N. Harakeh, T. Inomata, J. Janecke, S. Nakayama, A. Tamii, M. Tanaka, H. Toyokawa, W. Uijen, M. Yosoi, *Phys. Rev. Lett.* **82**, 3216 (1999).
- [11] V.E. Starodubsky, N.M. Hintz, *Phys. Rev.* **C49**, 2118 (1994).
- [12] W.M. Bugg, G.T. Condo, E.L. Hart, H.O. Cohn, R.D. McCulloch, *Phys. Rev. Lett.* **31**, 475 (1973).
- [13] M. Wade, V.G. Lind, *Phys. Rev.* **D14**, 1182 (1976).
- [14] G. Fricke, C. Bernhardt, K. Heilig, L.A. Schaller, L. Schellenberg, E.B. Shera, C.W. De Jager, *At. Data Nucl. Data Tables* **60**, 177 (1995).
- [15] H. de Vries, C.W. de Jager, C. de Vries, *At. Data Nucl. Data Tables* **36**, 495 (1987).
- [16] E. Oset, P. Fernandez de Cordoba, L.L. Salcedo, R. Brockmann, *Phys. Rep.* **188**, 79 (1990).
- [17] R. Smolańczuk, private communication.
- [18] Y.K. Gambhir, S.H. Patil, *Z. Phys.* **A324**, 9 (1986).
- [19] S. Wycech, *Nucl. Phys.* **B**, *Proceedings of the Sixth Biennial Conference on Low-Energy Antiproton Physics, Venice 2000*, to be published.
- [20] R. Schmidt, A. Trzcińska, T. Czosnyka, T. von Egidy, F.J. Hartmann, J. Jastrzębski, B. Ketzer, M. Kisieliński, B. Kłos, P. Lubiński, P. Napiorkowski, L. Pieńkowski, R. Smolańczuk, E. Widmann, to be published.
- [21] B. Kłos, PhD Thesis, Silesian University, Katowice 2000, unpublished.
- [22] R. Schmidt, F.J. Hartmann, T. von Egidy, T. Czosnyka, J. Iwanicki, J. Jastrzębski, M. Kisieliński, P. Lubiński, P. Napiorkowski, L. Pieńkowski, A. Trzcińska, J. Kulpa, R. Smolańczuk, S. Wycech, B. Kłos, K. Gulda, W. Kurcewicz, E. Widmann, *Phys. Rev.* **C58**, 3195 (1998).
- [23] F. Hofmann, H. Lenske, *Phys. Rev.* **C57**, 2281 (1998).